Research Square

Preprints are preliminary reports that have not undergone peer review.
They should not be considered conclusive, used to inform clinical practice,
or referenced by the media as validated information.

A TTN-mutation-associated gene signature for prognostic prediction of hepatocellular carcinoma

Yanqing Bi
Public Health College, Inner Mongolia Medical University
Rong Huang
Chinese Academy of Sciences
ziying Zhang
Basic Medical College, Inner Mongolia Medical University
Zixuan Tian
Public Health College, Inner Mongolia Medical University
min Liu
Public Health College, Inner Mongolia Medical University
Han Bao
Public Health College, Inner Mongolia Medical University
tao Yan
Public Health College, Inner Mongolia Medical University
Yuan Xia
Public Health College, Inner Mongolia Medical University
nan Zhang (17704713193@163.com)
Public Health College, Inner Mongolia Medical University
xingguang Zhang
Public Health College, Inner Mongolia Medical University

Research Article

Keywords: TTN mutation, gene signature, prognosis, functional analysis, HCC

Posted Date: June 2nd, 2022

DOI: https://doi.org/10.21203/rs.3.rs-1665120/v2

License: This work is licensed under a Creative Commons Attribution 4.0 International License.
Read Full License

Abstract

Background: Mutation in titin (TTN), associated with a worsened prognosis, is among the most common genetic variants in human hepatocellular carcinoma. mRNA expression data and TTN mutation information from TCGA cohort were utilized to characterize a specific TTN-mutation-associated signature according to gene-expression differences between wild type (TTN-WT) and TTN-mutated (TTN-MUT) hepatocellular carcinoma (HCC) patients. In total, 189 differentially expressed genes (DEGs) potentially correlated with TTN mutation status were identified.

Methods: Five genes (VAX1, MMP3, CXCL5, TKTL1 and KCNA3), identified by univariate Cox regression and Kaplan-Meier survival analyses, constituted an independent OS prognostic gene signature in HCC patients. Depending on this gene signature, patients were grouped into high- and low-risk subgroups and a significant enrichment associated with immunity is detected between the risk groups. In addition, the high-risk group was associated with an abundance of macrophages and neutrophils, while the infiltration indices of T follicular helper cells, natural killer cells, and type 2 helper T cells (Th2) were lower compared to low-risk group. In the multivariate Cox regression model, the five-gene signature remained a significant predictor independent of other conventional clinical risk factors used for survival prediction in HCC patients. MMP3 and CXCL5 expression were further validated in HCC cell lines.

Results: We established a novel and unique TTN-mutation-related gene signature for survival outcome prediction for HCC patients.

Conclusion: Our research foundings display a specific mechanism of TTN mutation and hold promise for the identification of HCC patients with poor prognosis.

Introduction

Hepatocellular carcinoma (HCC) represents the 3rd major cause of tumor-associated deaths (8.3% of the total cancer mortality) and the sixth leading type of diagnosed malignancies (4.7% of total cases) as stated by Global cancer statistics of 2020(1). HCC is associated with rapidly increasing cancer-related mortality since the beginning of 2000s in the USA according to the Surveillance Epidemiology End Results (SEER) report, and if these trends continue, deaths will reach 1 million per year by 2025(2). The clinical outcome of HCC remains unsatisfactory despite the use of new therapeutic drugs in recent years, including sorafenib and Lenvatinib(3–5). It is worth mentioning that due to the genetic heterogeneity, patients with tumors of identical clinical stage and pathological type usually have different outcomes after the same treatment(6). Approximately a quarter of all HCCs harbour potentially actionable mutations, which are not clearly assessed(7). The association between genetic changes in HCC and its prognosis has not been systematically comprehensively evaluated. Therefore, an in-depth knowledge regarding the molecular mechanisms of HCC pathogenesis is extremely needed for the establishment of more effective drug targets and innovative experimental therapies.

Genomic instability is a common characteristic of HCC(8), and multiple mutated genes have been identified so far in HCC, such as TP53, TTN, CTNNB1, MUC16 and PCLO(9). TP53 mutation is reported to keep a relationship with tumor recurrence, chemotherapy resistance, and decreased OS of HCC patients(10). Titin (TTN), with the longest human coding sequence (11), is a type of structural protein found in striated muscles(12) and mutations happened in this gene usually cause familial hypertrophic cardiomyopathy(13). Recent studies suggest that TTN is frequently detected in numerous solid tumors. Although potential mechanisms were unknown, TTN functions to increase TMB and respond to immune checkpoint blockade (ICB) objectively(14). TTN mutations, mainly non-synonymous mutations happened in its coding regions(11), are also one of the most common mutations in HCC(15). The TTN mutation has an association with the tumor immune micro-environment(11, 16). However, to date, a comprehensive understanding of the specific pathological characteristics and abnormal biological functions related to TTN mutations in HCC is lacking. In addition to the trait in solid tumors, we hypothesized that the the liver cancer microenvironment might influence the OS of HCC patients harboring TTN mutation. We evaluated the potential clinical application of TTN mutation status for prognostic stratification. Therefore, we established a five-gene signature affected by TTN mutation status for prediction of survival in patients with hepatocarcinoma.

Materials And Methods

Statement

TCGA and GEO belong to public databases. The patients involved in the database have obtained ethical approval. Users can download relevant data for free for research and publish relevant articles. Our study is based on open source data, so there are no ethical issues and other conflicts of interest. All methods were carried out in accordance with relevant guidelines and regulations.

Mutation Analysis

Mutation data for 364 HCC patients were retrieved from MAF files in the TCGA Somatic Mutation database (http://tcga-data.nci.nih.gov/tcga/). Firstly, all detected somatic mutations in the cohort were imported for mutation analysis. Next, on the basis of clinical data and transcriptome profiles, we excluded those individuals without complete information and effective survival time. The final data for somatic mutations were mapped in Mutation Annotation Format (MAF) by “maftoools” in R that contains most of the commonly used analysis as well as visualization modules about tumor genomic studies.

Identification of differentially expressed genes (DEGs)

Clinical data and the corresponding mRNA raw data, including 424 samples were retrieved from TCGA LIHC database. “DESeq2” in R was used to determine DEGs, and cut-off points were |log2-fold change (FC)| 1.0 and padj 0.05. The Draw Venn Diagram (http://bioin formatics.psb.ugent.be/webtools/Venn/) web-access tool was used to identify common DEGs.

GO and KEGG analyses of DEGs

GO (gene ontology) enrichment analysis was conducted based on GO molecular functions (GO MF), GO cellular component (GO CC), and GO biological processes (GO BP) for specific DEGs using R package clusterProfiler(v3.12.0). Meanwhile, KEGG analysis of DEGs was conducted using the same R package as GO enrichment analysis. A threshold to adjusted p-value <0.05 was used.

Cox regression Analyses

Clinical data and mRNA expression data from 374 HCC tissues were retrieved from TCGA (https://www.cancer.gov/). First, we used “survival’ in R to perform univariate-Cox regression analyses to screen DEGs correlated with OS in the training set. Clinicopathological factors and risk scores related to OS were assessed by univariate Cox regression analyses. Significant factors (p<0.05) were analyzed by multivariate Cox proportional hazard regression analyses to assess the clinical independence and predictive performance of our model.

Gene set enrichment analysis (GSEA)

To identify different signaling pathways between the subgroups, the GSEA v4.0.3 software was used for GSEA. Hallmark gene sets (h.all.v6.0.symbol.gmt) from the Molecular Signatures Database were used for annotation (17). FDR adjusted $p < 0.05$ and $|NES| \geq 1.5$ were the thresholds for significance.

Survival analysis

To assess the prognostic effect of DEGs, we performed univariate Cox regression and Kaplan-Meier (KM) analyses using R packages “survival” and “survminer”. The continuous variables were assigned into higher and lower groups based on the ideal cut-off point as established by the surv cutpoint function of “survminer” in R. Correlations between variables and OS or DFS of HCC patients in TCGA cohort were evaluated by Kaplan-Meier. The significance threshold was p <0.05.

Immune cell abundance prediction

Infiltrating immune cells, major components of the immune response in many solid tumours, play indispensable roles in immunotherapy. ImmuCellAI (http://bioinfo.life.hust.edu.cn/web/ImmuCellAI/) was used to determine the richness of 24 types of immune cells in samples with different risk scores. First, we upload the gene expression data to the website, next select ‘immune cell abundance in the sample’, after which the relative abundance of every type of immune cell in the samples was determined. Infiltration levels of immune cells in high- and low-risk groups were downloaded and visualized by R software.

Cell culture and quantitative real-time PCR (qRT-PCR)

HCC cell lines (PLC and HepG2) were procured from the Cell Resource Center of Peking Union Medical College (Beijing, China). The normal human liver cell line (LO2) and the HCC cell line (Huh7) were acquired from the China Cell Bank (Shanghai, China). Cells were grown in 10% FBS (Ausbian, Australia)-

supplemented DMEM (Gibco, Waltham, MA, USA) with 100 U/mL penicillin/0.1 mg/mL streptomycin. Incubation was done at 37 °C in a humid 5% CO2 environment. After thawing, cells were used for 15 passages. The Trizol reagent (Invitrogen, Carlsbad, CA , USA) was used for total RNA extraction from cells, after which cDNA synthesis was performed using 2μg of RNA and the RevertAid First Strand cDNA Synthesis Kit (Thermo Fisher Scientific). For each target sequence, qRT-PCR was conducted in triplicates using PowerUpTM SYBRTM Green Master Mix (Appliedbiosystems by Thermo Fisher Scientific) on a CFX ConnectTM Real-Time System (Biorad). The expressions of target genes were determined by $2^{-\Delta\Delta CT}$ approach and the internal control was human β-actin. Triplicates were performed for every sample and each experiment was repeated thrice. The primers used in this assay were: β-actin_F: 5'-CATGTACGTTGCTATCCAGGC-3'；β-actin_R: 5'-CTCCTTAATGTCACGCACGAT-3'；CXCL5_F: 5'-TGTGCAATTAACAAAGCTACTGC-3'；CXCL5_R: 5'-AGGCATCTAAAAAGCTCAGCAA-3'；MMP3_F: 5'-CACTCACAGACCTGACTCGG-3'；MMP3_ R: 5'-GAGTCAGGGGGAGGTCCATA-3'.

Results

Mutations in HCC

Mutations in each sample were presented in waterfall plot, and dissimilar colors indicate different mutation types. TP53, CTNNB1, and TTN were the commonly mutated genes (Supplementary Fig S1A). Missense single-nucleotide polymorphisms (SNPs), as well as C >T mutations, respectively, accounted for most of the categories (Supplementary Fig S1B–1D). Calculating mutation of every sample, median and maximum of mutations were 74.5 and 1250 separately (Supplementary Fig 1E). Moreover, counts of every variant type in dissimilar samples were presented informed of a box plot (Supplementary Fig 1F). Among the 364 HCC patients, TTN, CTNNB, TP53, MUC1, AL, PCLO, RYR2, MUC4, ABCA1 and APOB were the top 10 mutated genes (Supplementary Fig S1G).

Construction of the TTN mutation-associated prognostic signature in HCC patients

DEGs between the adjacent non-cancerous and HCC tissues were compared. Based on padj < 0.05 and |log2 FC| > 1 thresholds, 5977 DEGs were obtained. The volcano plot shows the DEGs (Figure 1A). As the second frequently mutated genes, TTN-mutation status was closely linked to HCC. Therefore, DEGs were explored between TTN mutated and wild-type groups. In summary, 19 upregulated and 330 down-regulated genes were found (Fig 1B). In total, 189 genes were differentially expressed in HCC samples, relative to normal samples (Fig 1C). To assess DEGs associated with OS outcomes in HCC patients, K-M and univariate Cox regression analyses were conducted among the 189 genes. At p < 0.05, 29 and 13 genes were identified, respectively (Fig 1D, 1E). As shown in Figure 1F, The VENN plot showed the common 5 prognostic associated genes (KCNA3, VAX1, MMP3, CXCL1 and TKTL1) in two analysis methods. According to the scores calculated by the risk assessment model, HCC patients were allocated into a high- and low-risk group (Fig 2A-2C). High risk patients had markedly worse DFS and OS outcomes relative low risk patients based on K-M analysis ((Fig 2D, 2E).

Kaplan-Meier analyses of survival outcomes based on the TTN mutation status

In addition to prognostic capacities of the five-gene signature, TTN-mutation groups were markedly negatively correlated with DFS and OS outcomes in HCC patients (Fig 3A, 3B). To investigate the TTN-mutation dependence of the five-gene signature, patients with HCC were allocated into high- and low-risk groups, respectively, in both TTN-mutation and wild type groups. Kaplan-Meier DFS curves and OS curves of the high- and low-risk groups based on the five-gene signature shared the same trends in the TTNWT and TTNMUT HCC cohorts, with high-risk groups had markedly poor outcomes (Fig 3C, 3D).

Enrichments of DEGs in high- and low-risk groups

The top 10 GO analyses results and KEGG analyses results are shown in a bar plot. Interestingly, DEGs were highly enriched in various immune-receptor associated BPs, including immune receptor activity and receptor ligand activity. KEGG pathway analyses showed high expression of genes relating to cytokine-cytokine receptor interaction pathway (Fig 4A). Furthermore, we conducted the GSEA enrichment analysis according to the riskscore level and some gene sets associated with cancer were markedly gathered in high-risk HCC patients, including “MYC targets V2”, “DNA repair”, “oxidative phosphorylation”, “MYC targets V1”, “glycolysis”, “G2M checkpoint”, “E2F targets”, “reactive oxygen species pathway”, “unfolded protein response” (Fig 4B).

Immune cell infiltrations

Tumor-infiltrating immune cells are the main components of the tumor microenvironment and play an important role in the occurrence, progression or metastasis of tumors. Therefore, assessing the potential correlation between different levels of immune cell infiltration in HCC enables observation of components and immune mechanisms that modulate the tumor microenvironment to influence antitumor immunity. To further characterize the complex immune status in solid tumors, ImmuCellAI was used for the prediction of the abundance of 24 immune cell types in high- and low-risk HCC patients based on RNA-Seq data. The abundance information of various taxonomic groups in each sample were shown in Fig 5A. The abundances of several tumor-immune cell types, including Tfh、Th2、MAIT、Tr1、nTreg, between high-and low-risk HCC patients were markedly different (Fig 5B). What’s more, immune cell abundances were moderately to highly associated (Fig 5C). The abundance of CD4 naive T cells, exhausted T cells (exhausted), cytotoxic T cells(cytotoxic), Type 1 regulatory T cells (Tr1), natural regulatory T (nTreg), induced regulatory T (iTreg), type 2 helper T cells (Th2), mucosal-associated invariant T cells (MAIT), central memory T cells, T cells follicular helper (Tfh), dendritic cells (DC), monocytes, natural killer cells (NK), CD4 T cells and CD8 T cells were generally high in low-risk group than in high-risk group. Contrastingly, the abundance of macrophages, Th17, and neutrophils were low in low-risk relative to the high-risk group (Fig 5D).

Correlations between the five-gene signature and clinic-pathological features

We next explored the independence of the risk score from the five-gene signature in regard to traditional prognostic indicators. Through univariate Cox regression analyses, M stage, T stage, TNM stage, and Risk score were markedly related with OS in HCC patients (Fig 6A). The above factors were subjected to multivariate Cox regression analyses, and the risk score was established to be an independent prognostic marker for HCC (Fig 6B). The risk score prediction model tended to exhibit better discriminative performance than other clinical factors (Fig 6C).

Verification of gene expressions in HCC cell lines

To validate the credibility of the gene signature, we evaluated CXCL5, VAX1, TKTL1, KCNA3 and MMP3 expression levels by RT-qPCR in human HCC and normal hepatocyte cell lines. Compared with normal cell line, MMP3 and CXCL5 mRNA expression were significantly higher in tumor cell lines （$p<0.05$(Fig 7).

Dissicussion

Hepatocellular carcinoma ranks the 2nd most common cause of tumor-associated death around the world, with a steady rise of incidence every year(18). The majority of treatments on early stage hepatocarcinoma patients include surgical resection, systemic pharmacological treatment, transplantation, transcatheter arterial chemoembolization, ablation therapies and radiotherapy currently(19). The overall five-year survival rate still ranges between 50% and 70%(20). Due to complex etiologic factors and high heterogeneity of HCC, the prognostic prediction of HCC is challenging. Due to the limited therapeutic options for HCC, it is important to develop new prognostic models.

We comfirmed that TTN has the second highest mutation frequency in liver cancer. In line with previous reportes, TTN mutation was frequently detected in many kinds of cancers, such as advanced non-small-cell lung cancer (NSCLC)(11), hepatocarcinoma(HCC)(19), head and neck squamous cell carcinoma (HNSCC)(21). Then, we identified 189 differently expressed genes between 50 normal liver tissues and 374 HCC tissues associated with TTN mutation. Then, we obtained five key genes (TKTL1, VAX1, KCNA3, MMP3 and CXCL5) directly related to prognosis via univariate Cox regression analyses and K-M survival analyses to form a risk signature with the potential for being an independent prognostic factor. Through the risk formula, we determined risk scores for every patient and assigned them into high/low-risk groups based on median risk score. High-risk group patients were associated with poorer outcomes. Next, Functional enrichment analyses were conducted to assess differences in some key signaling pathways and biological processes between TCGA LIHC cohort subgroups. GO and KEGG analysis revealed some immune cell-specific pathways and biological processes. Tumor-infiltrating immune cells, major TME components, have been widely investigated these last years. As reported, certain subtypes of tumor-infiltrating immune cells could be an indication of response to immunotherapies and OS for various solid tumor types(22–26). Furthermore, we predicted an relative abundance of the 24 types of immune cells using ImmuCellAI and found that patients with higher neutrophils and macrophages infiltration are at high risk of HCC while patients with higher abundance of T follicular helper cells、T cells CD8、dendritic cells and natural killer cells are at low risk of HCC. It is wellknown that T cells-mediated cell immune

responses play vital roles in anti-tumor immune responses(27, 28). As reported, high-risk LUAD patients had lower fractions of T cells follicular helper and T cells CD4 relative to low-risk patients(22). Keeping with this, our risk model demonstrates the essential role of tumor-infiltrating immune cells to define the HCC angiogenesis, invasion, and progression, with poor prognostic outcomes.

Clinical TNM, T, and M stages as well as Risk score markedly affected OS outcomes for HCC patients, and further analysis implied that the five-gene signature is an independent prognostic indicator for predicting a poor prognostic outcomes in HCC patients. This gene signature provided a robust approach to assess the model's predictive performance, and favor for outcome prediction and treatment decision. CXCL5 is a member of a proangiogenic subgroup of the CXC-type chemokine family of small, secreted proteins. It has been found that CXCL5 is overexpressed in various cancers, including gastric(28), prostate(29, 30), endometrial(31), squamous cell(32), pancreatic cancer(30, 33, 34), and hepatocellular carcinoma. Elevated CXCL5 levels are correlated with local invasion, advanced tumor stages, and metastatic potential. CXCL5 activates PI3K-Akt and ERK1/2 signaling pathways in HCC cells, promoting proliferation, migration and invasion (35). The expression level of CXCL5 in HCC is significantly higher than that in normal liver tissue, and the expression level of CXCL5 mRNA and protein is related to intrahepatic metastasis, portal vein tumor thrombus, and poor differentiation (36). One study showed that a long-term increase in CXCL5 was associated with a promotion of NAFLD progression to HCC in males (37). Another study showed that overexpression of CXCL5 in HCC cells has a higher metastatic potential, which also suggested that CXCL5 may play an important role in the migration of HCC .(38)This study find that overexpression of CXCL5 in hepatocellular carcinoma is associated with TTN mutation.

Matrix metalloproteinase (MMP)-3 function as a protease involved in cancer progression and tissue remodeling(39), certain genes like Cathepsin Z (CTSZ) (40), Cyclophilin A(41), demonstrate an oncogenic role in HCC by elevating extracellular matrix remodeling-associated proteins such as MMP2/3/9. Downregulated MiR-30a-3p regulates HCC cell functions by suppressing vimentin and MMP3 levels and restoring E-cadherin levels(42). Transketolase-like protein 1 (TKTL1), a key characteristic of tumor cells, coordinates glucose utilization with cell physiology, and its high expression indicates poor prognosis in colorectal cancer patients with synchronous liver metastases(43). Silencing expression of TKTL1 by RNAi suppresses human hepatoma cell proliferation(44). VAX1 encodes a homeodomain transcription factor mainly functions in optic chiasm and eye development(45). Until now, few studies haved reported its role in cancer. The voltage-gated potassium channel Kv1.3 (KCNA3) was detected at a very high level in various chronic activated T-cell diseases (46–48). KCNA3 has been implicated in cancer cell proliferation and apoptosis in several types of tumors. In addition, studies have shown that the amount of KCNA3 expression varies with the stage of cancer (49), and KCNA3 knockdown significantly inhibits cell proliferation and increases cell apoptosis (50). Moreover, KCNA3 act as a mediator of prognosis in HCC, yet the expression and molecular mechanisms by which KCNA3 exerts were still unknown(51). Taken together, our findings are in tandem with those of other studies and the five-gene signature associated with TTN mutation would be worthwhile for identifying novel therapies to improve long-term patient outcome in the future. It is expected to be a potential biomarker and therapeutic target to change the prognosis of HCC patients.

Declarations

Ethics approval and consent to participate.

Not applicable.

Consent for publication

Not applicable.

Data Availability Statement

All data used during the study appear in the submitted article.

Competing interests

The authors declare that they have no competing interests.

Funding

The study was supported by the Shanxue Talents project of Zhiyuan Talent Plan of Inner Mongolia Medical University [grant numbers ZY0201025]; The Program for Young Talents of Science and Technology in Universities of Inner Mongolia Autonomous Region [grant numbers NJYT22008]; The Inner Mongolia Health Science and Technology Project [grant numbers 202201227].

Author contributions

All authors contributed to the study conception and design. Material preparation, data collection and analysis were performed by Xingguang Zhang, Nan Zhang and Rong Huang. The first draft of the manuscript was written by Yanqing Bi and all authors commented on previous versions of the manuscript. All authors read and approved the final manuscript.

Acknowledgements

Not applicable

References

1. Sung HA-O, Ferlay J, Siegel RA-O, Laversanne M, Soerjomataram I, Jemal A, et al. Global Cancer Statistics 2020: GLOBOCAN Estimates of Incidence and Mortality Worldwide for 36 Cancers in 185 Countries. (1542–4863 (Electronic)).
2. Rahib L, Smith BD, Aizenberg R, Rosenzweig AB, Fleshman JM, Matrisian LM. Projecting cancer incidence and deaths to 2030: the unexpected burden of thyroid, liver, and pancreas cancers in the United States. (1538–7445 (Electronic)).

3. Eso YA-Ohoo, Marusawa H. Novel approaches for molecular targeted therapy against hepatocellular carcinoma. (1386–6346 (Print)).
4. Llovet JM, Montal R, Villanueva A. Randomized trials and endpoints in advanced HCC: Role of PFS as a surrogate of survival. (1600 – 0641 (Electronic)).
5. Reig M, da Fonseca LG, Faivre S. New trials and results in systemic treatment of HCC. (1600 – 0641 (Electronic)).
6. Lin DC, Mayakonda A, Dinh HQ, Huang P, Lin L, Liu X, et al. Genomic and Epigenomic Heterogeneity of Hepatocellular Carcinoma. (1538–7445 (Electronic)).
7. Llovet JA-O, Kelley RK, Villanueva AA-O, Singal AG, Pikarsky E, Roayaie S, et al. Hepatocellular carcinoma. (2056-676X (Electronic)).
8. Niu ZS, Niu XJ, Wang WH. Genetic alterations in hepatocellular carcinoma: An update. (2219–2840 (Electronic)).
9. Kong F, Kong D, Yang X, Yuan D, Zhang N, Hua X, et al. Integrative analysis of highly mutated genes in hepatitis B virus-related hepatic carcinoma. (2045–7634 (Electronic)).
10. Li S, Gao M, Li Z, Song L, Gao X, Han J, et al. p53 and P-glycoprotein influence chemoresistance in hepatocellular carcinoma. (1945 – 0508 (Electronic)).
11. Su C, Wang X, Zhou J, Zhao J, Zhou F, Zhao G, et al. Titin mutation in circulatory tumor DNA is associated with efficacy to immune checkpoint blockade in advanced non-small cell lung cancer. (2218–6751 (Print)).
12. Ciferri A, Crumbliss AL. The Assembling and Contraction Mechanisms of Striated Muscles. (2296–2646 (Print)).
13. Gerull B, Gramlich M Fau - Atherton J, Atherton J Fau - McNabb M, McNabb M Fau - Trombitas K, Trombitas K Fau - Sasse-Klaassen S, Sasse-Klaassen S Fau - Seidman JG, et al. Mutations of TTN, encoding the giant muscle filament titin, cause familial dilated cardiomyopathy. (1061–4036 (Print)).
14. Jia Q, Wang J, He N, He J, Zhu B. Titin mutation associated with responsiveness to checkpoint blockades in solid tumors. LID – 10.1172/jci.insight.127901 [doi] LID – 127901 [pii]. (2379–3708 (Electronic)).
15. Yin L, Zhou L, Xu R. Identification of Tumor Mutation Burden and Immune Infiltrates in Hepatocellular Carcinoma Based on Multi-Omics Analysis. (2296-889X (Print)).
16. Wang Z, Wang C, Lin S, Yu X. Effect of TTN Mutations on Immune Microenvironment and Efficacy of Immunotherapy in Lung Adenocarcinoma Patients. (2234-943X (Print)).
17. Subramanian A, Tamayo P Fau - Mootha VK, Mootha Vk Fau - Mukherjee S, Mukherjee S Fau - Ebert BL, Ebert Bl Fau - Gillette MA, Gillette Ma Fau - Paulovich A, et al. Gene set enrichment analysis: a knowledge-based approach for interpreting genome-wide expression profiles. (0027-8424 (Print)).
18. Li Z, Zhang H, Han J, Chen YA-Ohoo, Lin H, Yang T. Surface Nanopore Engineering of 2D MXenes for Targeted and Synergistic Multitherapies of Hepatocellular Carcinoma. (1521–4095 (Electronic)).

19. Wang R, Hu X, Liu X, Bai L, Gu J, Li QA-O. Construction of liver hepatocellular carcinoma-specific lncRNA-miRNA-mRNA network based on bioinformatics analysis. (1932–6203 (Electronic)).
20. Bruix J, Llovet JM. Major achievements in hepatocellular carcinoma. (1474-547X (Electronic)).
21. Jiang AM, Ren MD, Liu N, Gao H, Wang JJ, Zheng XQ, et al. Tumor Mutation Burden, Immune Cell Infiltration, and Construction of Immune-Related Genes Prognostic Model in Head and Neck Cancer. (1449–1907 (Electronic)).
22. Shi Y, Gao W, Lytle NK, Huang P, Yuan X, Dann AM, et al. Targeting LIF-mediated paracrine interaction for pancreatic cancer therapy and monitoring. Nature. 2019;569(7754):131–5.
23. Zhang J, Wang J, Qian Z, Han Y. CCR5 is Associated With Immune Cell Infiltration and Prognosis of Lung Cancer. (1556 – 1380 (Electronic)).
24. Miksch RA-O, Schoenberg MA-O, Weniger MA-O, Bosch F, Ormanns S, Mayer B, et al. Prognostic Impact of Tumor-Infiltrating Lymphocytes and Neutrophils on Survival of Patients with Upfront Resection of Pancreatic Cancer. LID - E39 [pii] LID – 10.3390/cancers11010039 [doi]. (2072–6694 (Print)).
25. Zhou R, Zhang J, Zeng D, Sun H, Rong X, Shi M, et al. Immune cell infiltration as a biomarker for the diagnosis and prognosis of stage I-III colon cancer. (1432 – 0851 (Electronic)).
26. Hermans IF, Ritchie Ds Fau - Yang J, Yang J Fau - Roberts JM, Roberts Jm Fau - Ronchese F, Ronchese F. CD8 + T cell-dependent elimination of dendritic cells in vivo limits the induction of antitumor immunity. (0022-1767 (Print)).
27. Peng F, Zhou J, Sheng W, Zhang D, Dong M. [Expression and significance of leukemia inhibitory factor in human pancreatic cancer]. Zhonghua Yi Xue Za Zhi. 2014;94(2):90–5.
28. Park JY, Park Kh Fau - Bang S, Bang S Fau - Kim MH, Kim Mh Fau - Lee J-E, Lee Je Fau - Gang J, Gang J Fau - Koh SS, et al. CXCL5 overexpression is associated with late stage gastric cancer. (0171–5216 (Print)).
29. Begley LA, Kasina S Fau - Mehra R, Mehra R Fau - Adsule S, Adsule S Fau - Admon AJ, Admon Aj Fau - Lonigro RJ, Lonigro Rj Fau - Chinnaiyan AM, et al. CXCL5 promotes prostate cancer progression. (1476–5586 (Electronic)).
30. Frick VO, Rubie C Fau - Wagner M, Wagner M Fau - Graeber S, Graeber S Fau - Grimm H, Grimm H Fau - Kopp B, Kopp B Fau - Rau BM, et al. Enhanced ENA-78 and IL-8 expression in patients with malignant pancreatic diseases. (1424–3911 (Electronic)).
31. Wong YF, Cheung Th Fau - Lo KWK, Lo Kw Fau - Yim SF, Yim Sf Fau - Siu NSS, Siu Ns Fau - Chan SCS, Chan Sc Fau - Ho TWF, et al. Identification of molecular markers and signaling pathway in endometrial cancer in Hong Kong Chinese women by genome-wide gene expression profiling. (0950–9232 (Print)).
32. Miyazaki H, Patel V Fau - Wang H, Wang H Fau - Edmunds RK, Edmunds Rk Fau - Gutkind JS, Gutkind Js Fau - Yeudall WA, Yeudall WA. Down-regulation of CXCL5 inhibits squamous carcinogenesis. (0008-5472 (Print)).

33. Wente MN, Keane Mp Fau - Burdick MD, Burdick Md Fau - Friess H, Friess H Fau - Büchler MW, Büchler Mw Fau - Ceyhan GO, Ceyhan Go Fau - Reber HA, et al. Blockade of the chemokine receptor CXCR2 inhibits pancreatic cancer cell-induced angiogenesis. (0304–3835 (Print)).
34. Li A, King J Fau - Moro A, Moro A Fau - Sugi MD, Sugi Md Fau - Dawson DW, Dawson Dw Fau - Kaplan J, Kaplan J Fau - Li G, et al. Overexpression of CXCL5 is associated with poor survival in patients with pancreatic cancer. (1525–2191 (Electronic)).
35. Zhou SL, Dai Z, Zhou ZJ, Wang XY, Yang GH, Wang Z, et al. Overexpression of CXCL5 mediates neutrophil infiltration and indicates poor prognosis for hepatocellular carcinoma. Hepatology. 2012;56(6):2242–54.
36. Liu Z, Yang L, Xu J, Zhang X, Wang B. Enhanced expression and clinical significance of chemokine receptor CXCR2 in hepatocellular carcinoma. J Surg Res. 2011;166(2):241–6.
37. Mirshahi F, Aqbi HF, Cresswell K, Saneshaw M, Coleman C, Jacobs T, et al. Longitudinal studies can identify distinct inflammatory cytokines associated with the inhibition or progression of liver cancer. Liver Int. 2020;40(2):468–72.
38. Xu X, Huang P, Yang B, Wang X, Xia J. Roles of CXCL5 on migration and invasion of liver cancer cells. J Transl Med. 2014;12:193.
39. Si-Tayeb K, Monvoisin A Fau - Mazzocco C, Mazzocco C Fau - Lepreux S, Lepreux S Fau - Decossas M, Decossas M Fau - Cubel G, Cubel G Fau - Taras D, et al. Matrix metalloproteinase 3 is present in the cell nucleus and is involved in apoptosis. (0002-9440 (Print)).
40. Wang J, Chen L Fau - Li Y, Li Y Fau - Guan X-Y, Guan XY. Overexpression of cathepsin Z contributes to tumor metastasis by inducing epithelial-mesenchymal transition in hepatocellular carcinoma. (1932–6203 (Electronic)).
41. Zhang M, Dai C Fau - Zhu H, Zhu H Fau - Chen S, Chen S Fau - Wu Y, Wu Y Fau - Li Q, Li Q Fau - Zeng X, et al. Cyclophilin A promotes human hepatocellular carcinoma cell metastasis via regulation of MMP3 and MMP9. (1573–4919 (Electronic)).
42. Wang W, Lin H, Zhou L, Zhu Q, Gao S, Xie H, et al. MicroRNA-30a-3p inhibits tumor proliferation, invasiveness and metastasis and is downregulated in hepatocellular carcinoma. (1532–2157 (Electronic)).
43. Peltonen R, Ahopelto K, Hagström J, Böckelman CA-O, Haglund C, Isoniemi H. High TKTL1 expression as a sign of poor prognosis in colorectal cancer with synchronous rather than metachronous liver metastases. (1555–8576 (Electronic)).
44. Zhang S, Yang Jh Fau - Guo C-K, Guo Ck Fau - Cai P-C, Cai PC. Gene silencing of TKTL1 by RNAi inhibits cell proliferation in human hepatoma cells. (0304–3835 (Print)).
45. Bharti K, Gasper M Fau - Bertuzzi S, Bertuzzi S Fau - Arnheiter H, Arnheiter H. Lack of the ventral anterior homeodomain transcription factor VAX1 leads to induction of a second pituitary. (1477–9129 (Electronic)).
46. Rangaraju S, Chi V Fau - Pennington MW, Pennington Mw Fau - Chandy KG, Chandy KG. Kv1.3 potassium channels as a therapeutic target in multiple sclerosis. (1744–7631 (Electronic)).

47. Beeton C, Wulff H Fau - Standifer NE, Standifer Ne Fau - Azam P, Azam P Fau - Mullen KM, Mullen Km Fau - Pennington MW, Pennington Mw Fau - Kolski-Andreaco A, et al. Kv1.3 channels are a therapeutic target for T cell-mediated autoimmune diseases. (0027-8424 (Print)).
48. Kundu-Raychaudhuri S, Chen YJ, Wulff H, Raychaudhuri SP. Kv1.3 in psoriatic disease: PAP-1, a small molecule inhibitor of Kv1.3 is effective in the SCID mouse psoriasis–xenograft model. (1095–9157 (Electronic)).
49. Jang SH, Kang KS, Ryu PD, Lee SY. Kv1.3 voltage-gated K(+) channel subunit as a potential diagnostic marker and therapeutic target for breast cancer. BMB Rep. 2009;42(8):535–9.
50. Wu J, Zhong D, Wu X, Sha M, Kang L, Ding Z. Voltage-gated potassium channel Kv1.3 is highly expressed in human osteosarcoma and promotes osteosarcoma growth. Int J Mol Sci. 2013;14(9):19245–56.
51. Tian Z, Wang Z, Chen Y, Qu S, Liu C, Chen F, et al. Bioinformatics Analysis of Prognostic Tumor Microenvironment-Related Genes in the Tumor Microenvironment of Hepatocellular Carcinoma. (1643–3750 (Electronic)).

Figures

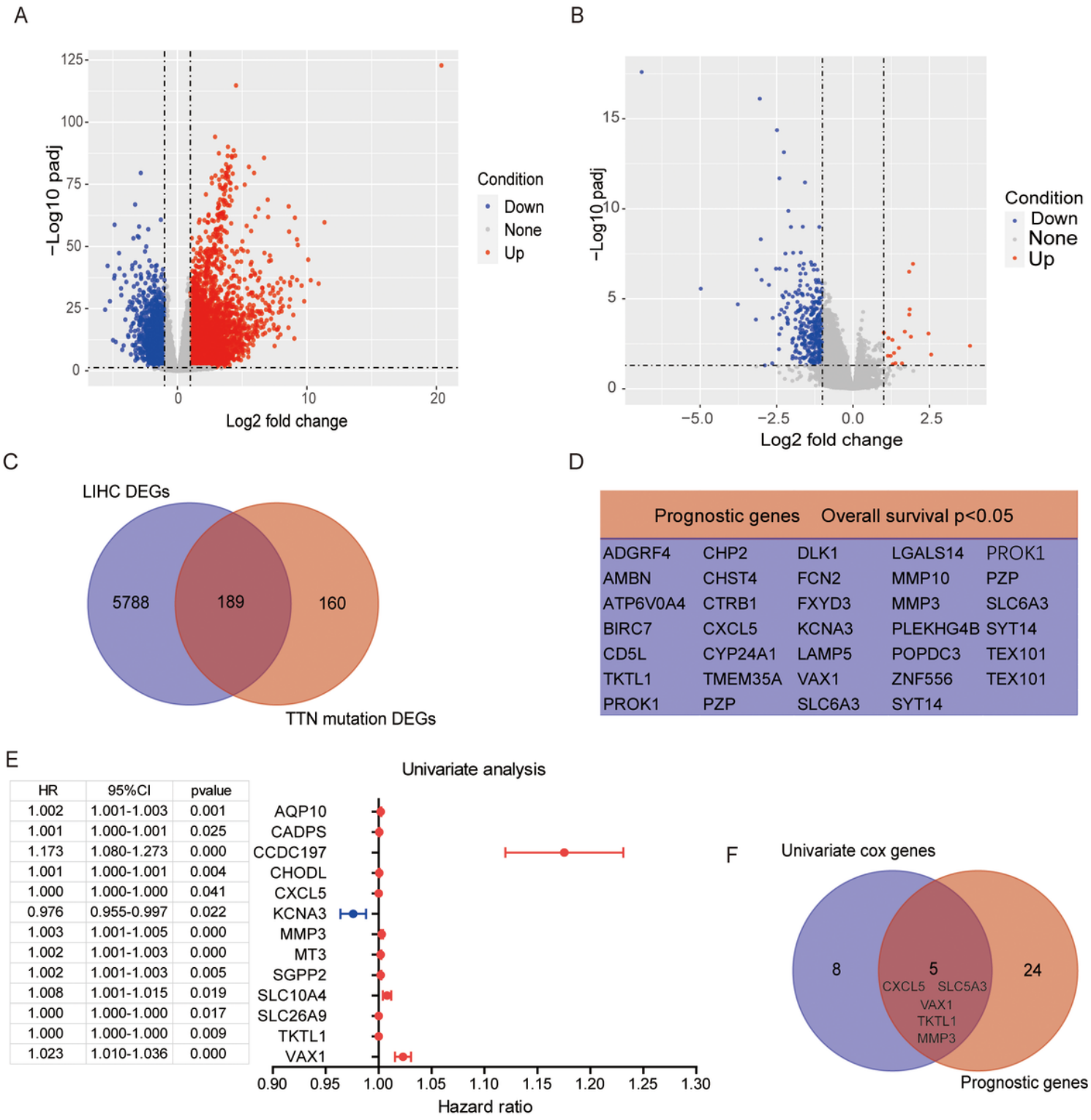

Figure 1

Analysis of DEGs in HCC patients with/without TTN mutations.

(A)Volcano plots for DEGs between HCC and the adjacent normal samples. (B) Volcano plots for DEGs between TTN-mutations and TTN wild-type groups. (C) Venn diagram to determine DEGs between cancer and the adjacent normal tissues that were associated with TTN mutation. (D) List of genes significantly associated with OS in 189 DEGs identified in HCC patients with and without TTN mutations. (E) Forest

plot for significant variables in univariate Cox regression analyses of 189 DEGs between wild-type and TTN-mutation group associated with liver cancer (F) Venn diagram to identify the common 5 prognostic associated genes associated with TTN mutation.

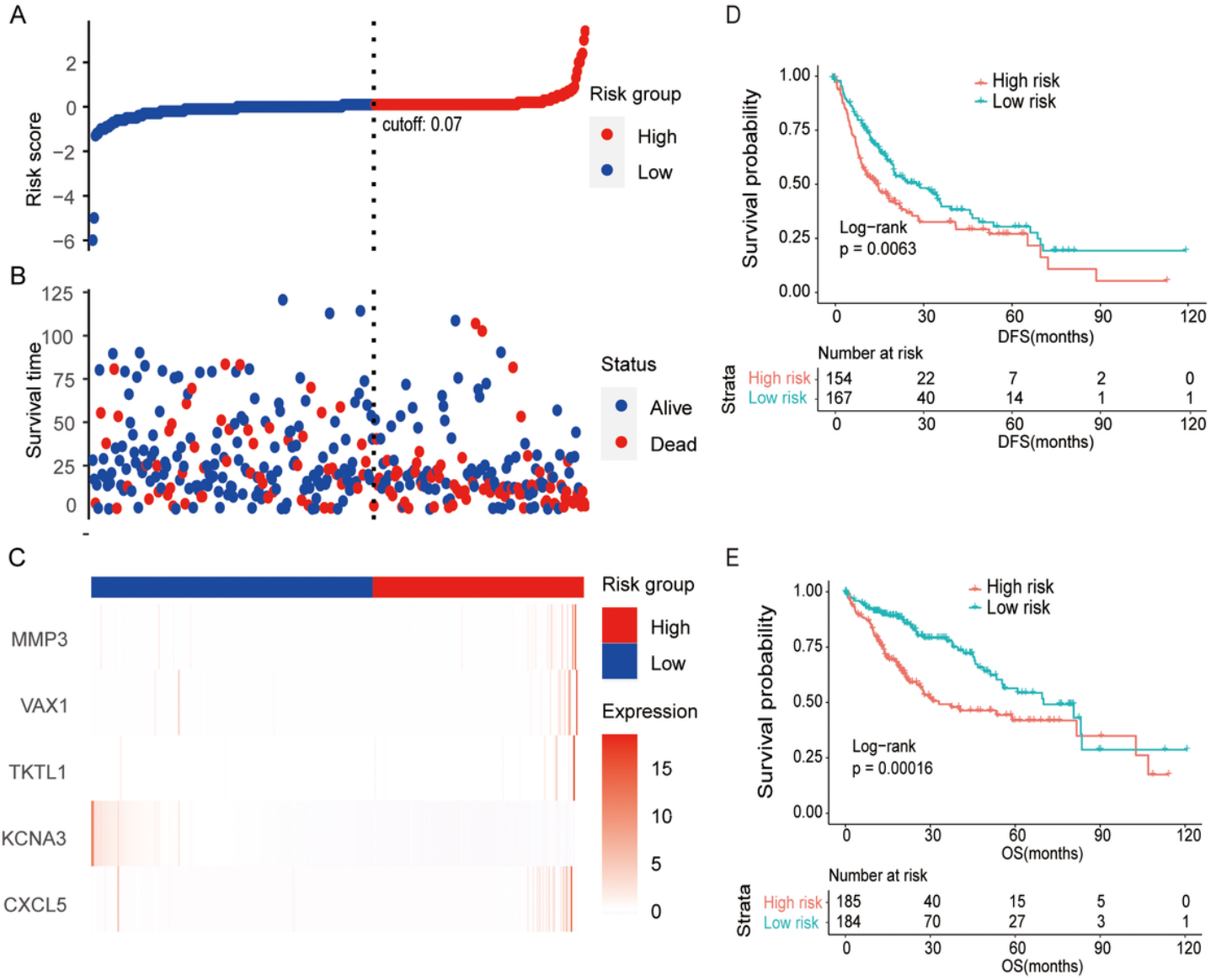

Figure 2

Establishment of the prognostic model.

(A)Risk score distributions with regards to the five-gene-signature. (B) Vital status of HCC patients in high- and low-risk groups. (C) Heatmap of the core five-gene levels in low and high-risk groups. (D-E). Kaplan-Meier survival curves for relative DFS and OS outcomes of high- and low-risk patients.

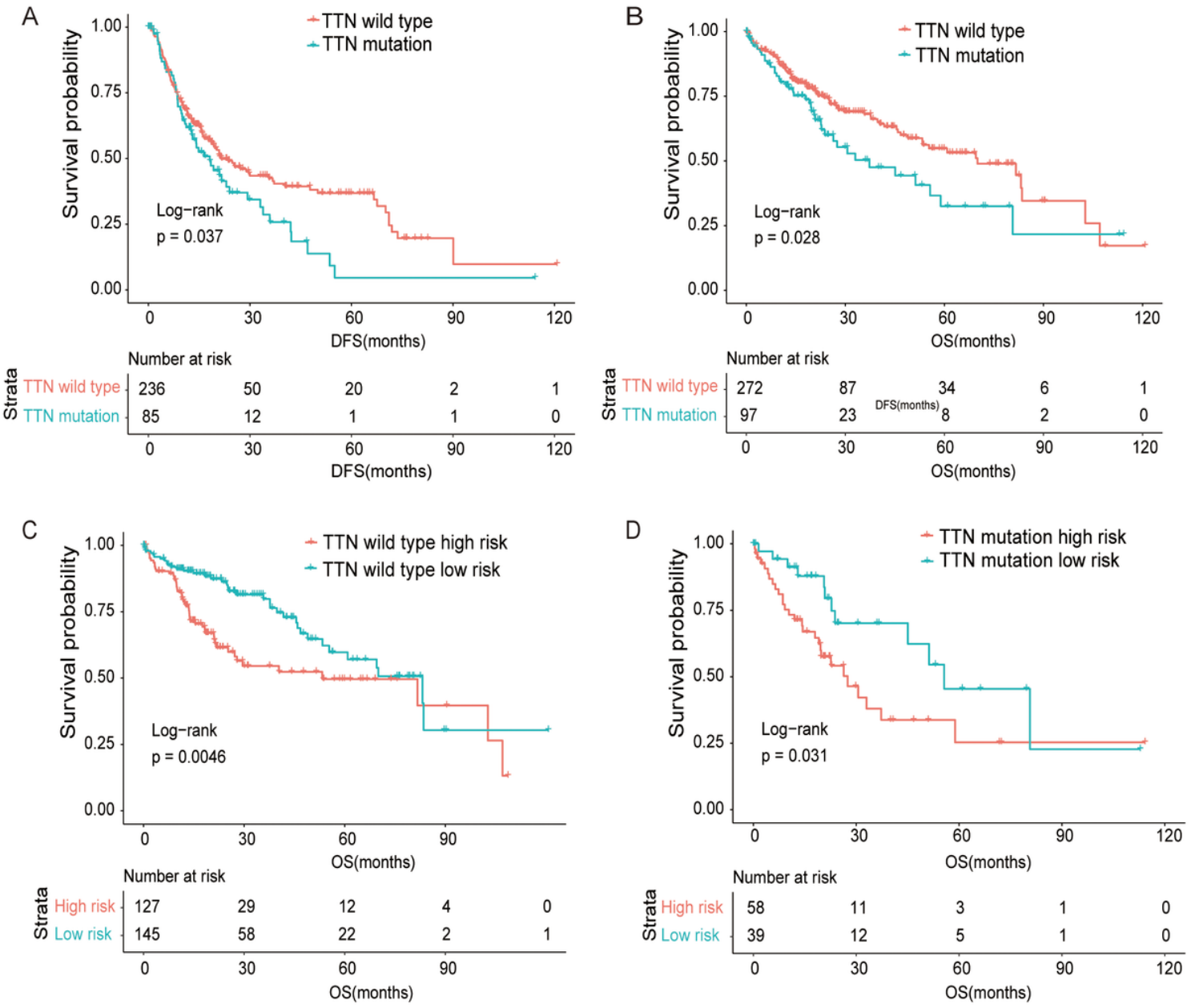

Figure 3

Kaplan-Meier analyses of specific variables.

(A-B). Kaplan-Meier analyses of DFS and OS based on TTN mutation status. (C-D). Kaplan-Meier curves for OS of HCC patients in high- and low-risk groups with different types of TTN mutations.

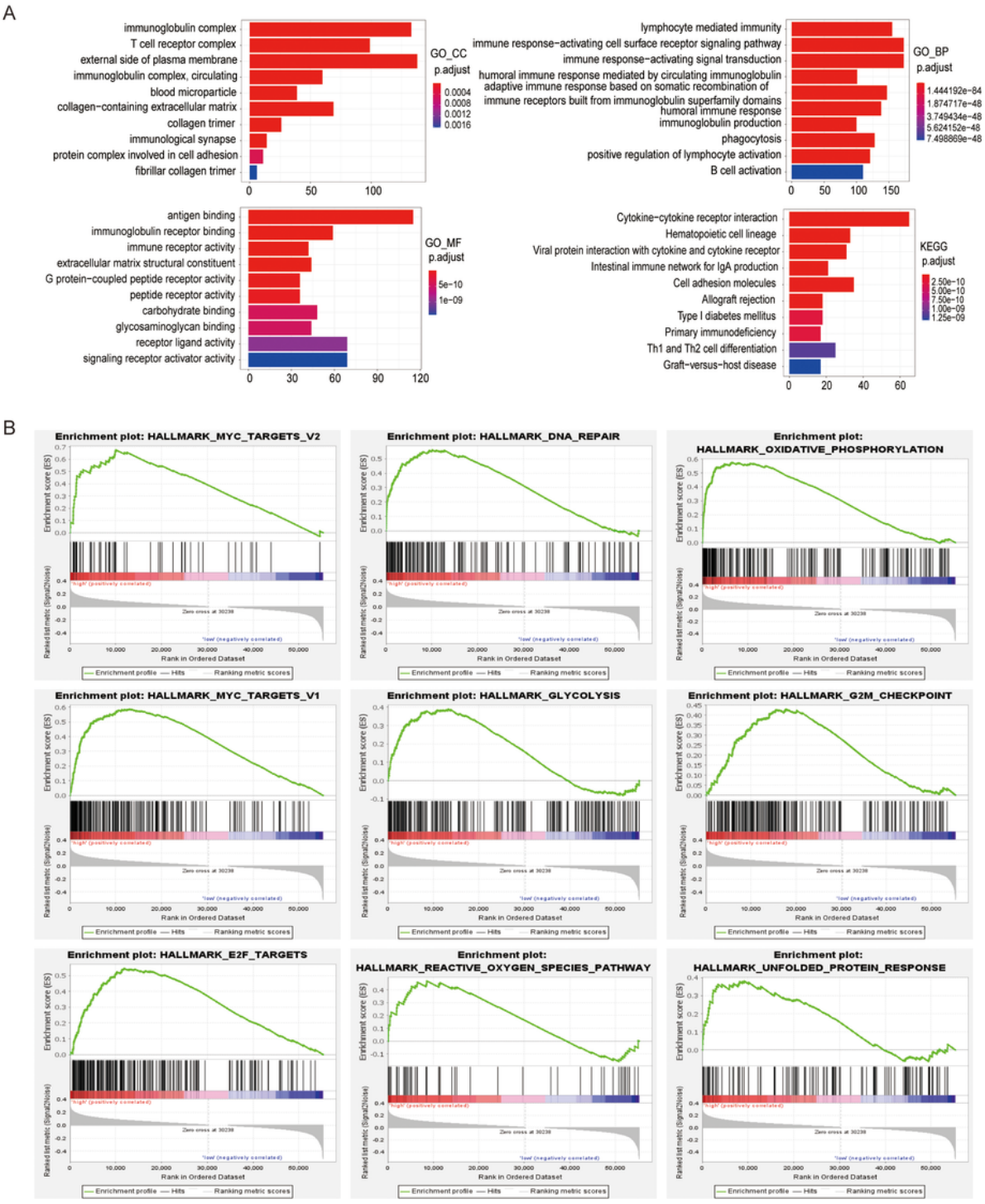

Figure 4

Pathway and process enrichment analyses of DEGs between high- and low-risk groups.

(A)GO and KEGG analyses across DEGs in high- and low-risk groups with regard to BPs, CCs, MFs and KEGG pathway. (B) GSEA was done to establish the marked hallmark gene sets in the high-risk and low-risk group.

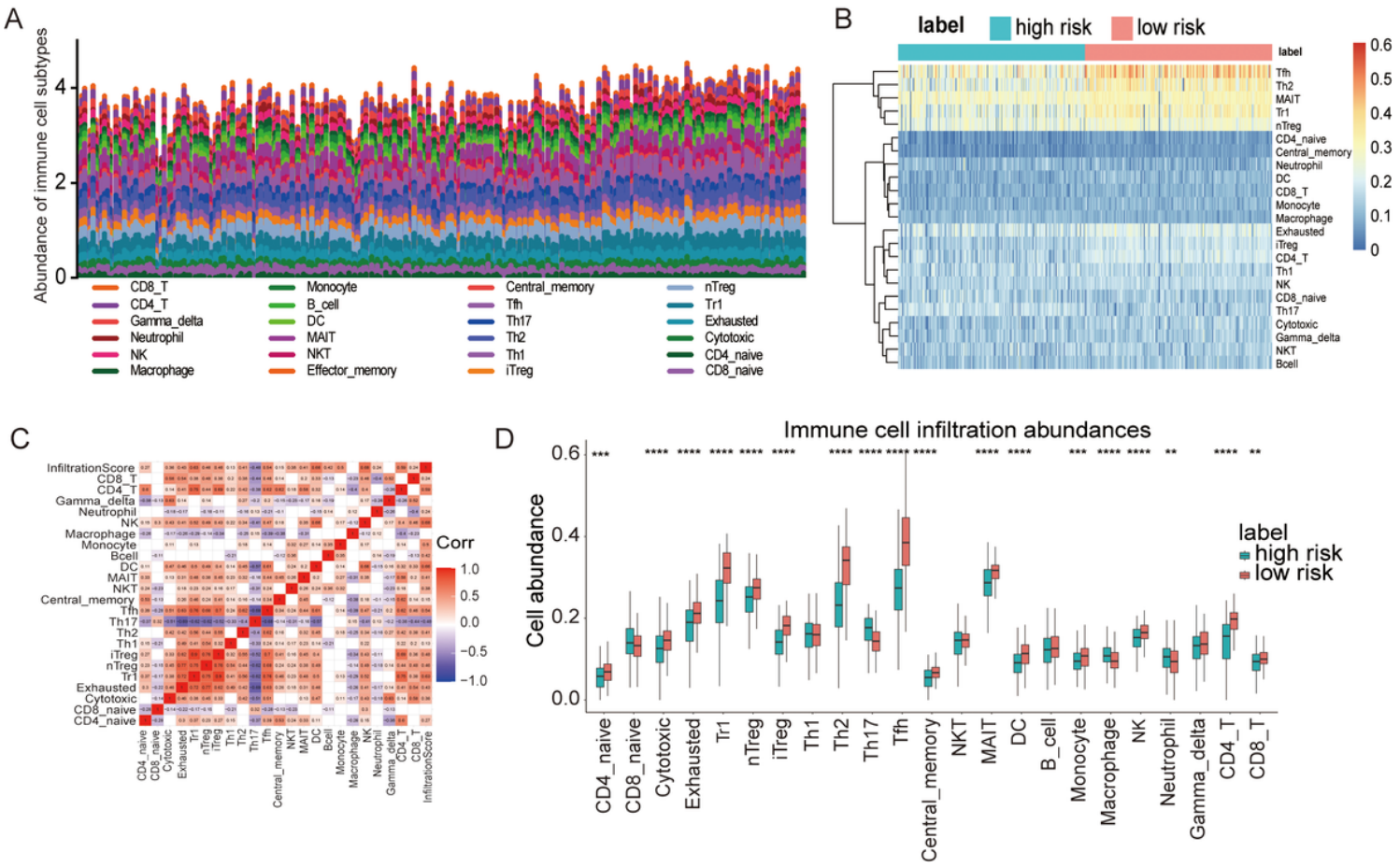

Figure 5

Infiltrating cell components as determined by ImmuCellAI.

Abundance of 24 types of immune cells in TCGA-LIHC cohorts. (B) Heatmap of sub-populations of immune cells in high- and low-risk groups. (C) Correlations matrix of immune cell proportions. (D) Immune cell richness between high- and low-risk groups.

A

HR	95%CI	pvalue
4.261	1.337-13.577	0.014
2.076	0.508-8.480	0.309
2.611	1.794-3.798	0
2.696	1.889-3.848	0
1.206	0.850-1.712	0.295
0.773	0.541-1.105	0.158
0.993	0.983-1.003	0.16
1.149	1.098-1.203	0

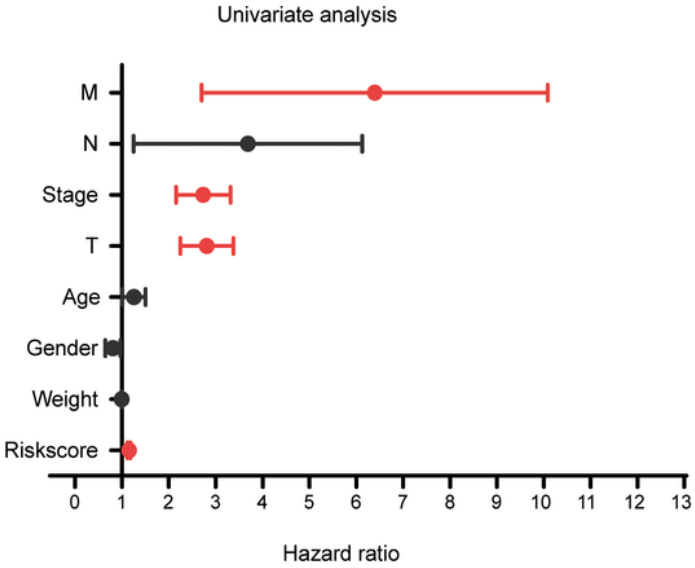

B

HR	95%CI	pvalue
2.151	0.659-7.024	0.205
2.01	0.275-14.699	0.491
1.472	0.201-10.799	0.704
1.199	1.104-1.302	0

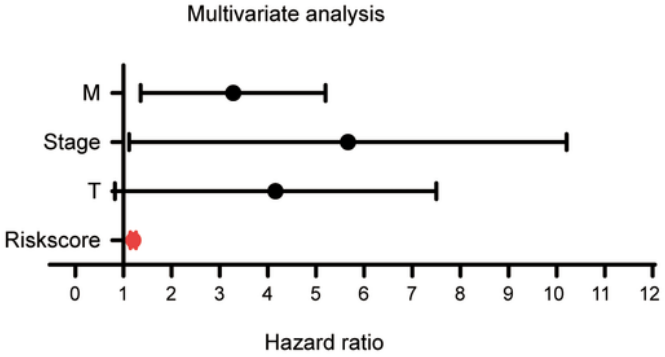

C

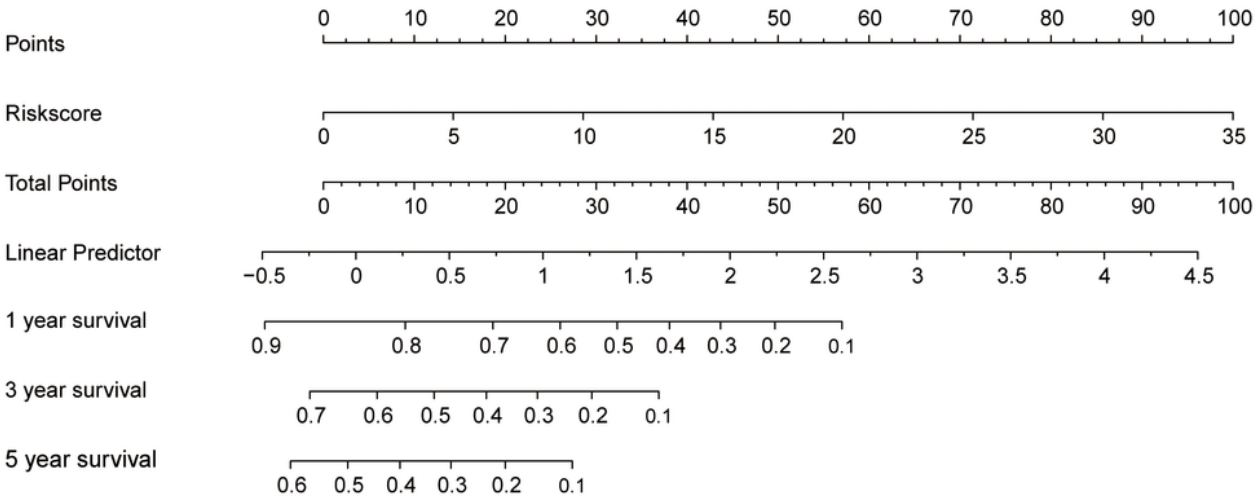

Figure 6

Correlations analyses between the five-gene signature and clinicopathological features.

(A-B) Univariate and multivariate Cox regression analyses of clinical features and risk signature with OS.
(C) Nomogram for prediction of HCC patients with 1-, 3- and 5-year OS.

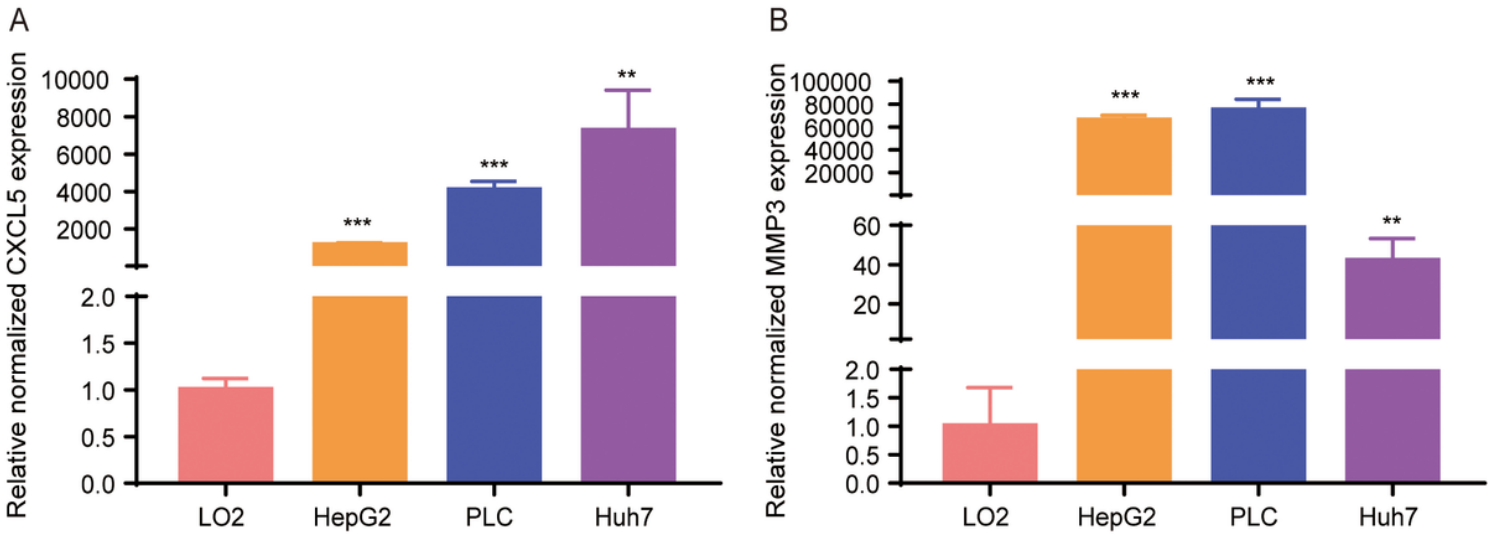

Figure 7

The mRNA levels of CXCL5 and MMP3 in HCC and normal liver cell lines by qRT-PCR.

(*$p \leq 0.05$; **$p \leq 0.01$;***$p \leq 0.001$)

Supplementary Files

This is a list of supplementary files associated with this preprint. Click to download.

- SupplementaryFigS1.tif